Published in final edited form as:

Sci Transl Med. 2020 October 28; 12(567): . doi:10.1126/scitranslmed.aaz4997.

Nonhuman primates exposed to Zika virus *in utero* are not protected against reinfection at one year postpartum

Kevin M. Vannella[1], **Sydney Stein**[1], **Mark Connelly**[1], **Joanna Swerczek**[2], **Emerito Amaro-Carambot**[3], **Elizabeth M. Coyle**[4], **Ashley Babyak**[1], **Clayton W. Winkler**[5], **Greg Saturday**[6], **Neville D. Gai**[7], **Dima A. Hammoud**[7], **Kimberly A. Dowd**[8], **Luis Perez Valencia**[1], **Marcos J. Ramos-Benitez**[1], **Jason Kindrachuk**[1,9], **Theodore C. Pierson**[8], **Karin E. Peterson**[5], **Jason M. Brenchley**[10], **Steve S. Whitehead**[3], **Surender Khurana**[4], **Richard Herbert**[2], **Daniel S. Chertow**[1,*]

[1]Emerging Pathogens Section, Critical Care Medicine Department, Clinical Center, National Institutes of Health, Bethesda, MD, USA; Laboratory of Immunoregulation, National Institute of Allergy and Infectious Diseases, National Institutes of Health, Bethesda, MD 20892, USA.

[2]Experimental Primate Virology Section, Comparative Medicine Branch, National Institute of Allergy and Infectious Diseases, National Institutes of Health, Poolesville, MD 20837, USA.

[3]Laboratory of Infectious Diseases, National Institute of Allergy and Infectious Diseases, National Institutes of Health, Bethesda, MD 20892, USA.

[4]Division of Viral Products, Center for Biologics Evaluation and Research, Food and Drug Administration, Silver Spring, MD 20993, USA.

[5]Laboratory of Persistent Viral Diseases, Rocky Mountain Laboratories, National Institute of Allergy and Infectious Diseases, National Institutes of Health, Hamilton, MT 59840, USA.

[6]Rocky Mountain Veterinary Branch, National Institute of Allergy and Infectious Diseases, National Institutes of Health, Hamilton, MT 59840, USA.

[7]Center for Infectious Disease Imaging, Radiology and Imaging Services, National Institutes of Health, Bethesda, MD 20892, USA.

[8]Laboratory of Viral Diseases, National Institute of Allergy and Infectious Diseases, National Institutes of Health, Bethesda, MD 20892, USA.

[9]Laboratory of Emerging Viruses, Department of Medical Microbiology, University of Manitoba, Winnipeg, MB R3E 0J9, Canada.

[*]Corresponding author. chertowd@cc.nih.gov.

Author contributions: M.C., J.K., S.S.W., R.H., and D.S.C. conceived and designed the longitudinal study; K.M.V., J.M.B., and D.S.C. conceived and designed the ZIKV reinfection study; E.A. and S.S.W. prepared and titrated the virus; E.A. designed and executed qPCR and $PRNT_{50}$ assays and analyzed the data; K.M.V., S.S., and D.S.C. designed and executed the ddPCR assay and analyzed the data; R.H., J.S., M.C., S.S., K.M.V., L.P.V., A.B., and D.S.C., designed and executed live animal procedures and observations as well as necropsy procedures; E.M.C. and S.K. designed and executed the surface plasmon resonance assay and analyzed the data; K.M.V., A.B., and J.M.B. designed and executed the T cell assays and analyzed the data; C.W.W., K.E.P., and G.S. performed immunostaining on tissues and evaluated histopathology; N.D.G. and D.A.H. executed and evaluated MRI; K.A.D., M.J.R., and T.C.P. designed and executed antibody-dependent enhancement experiments; K.E.P., S.S.W., T.C.P., and S.K. contributed reagents; K.M.V. wrote the manuscript, and S.S., J.K., T.C.P., K.E.P., and D.S.C. critically evaluated and edited the manuscript

Competing interests: The authors declare no competing interests.

[10]Barrier Immunity Section, Laboratory of Viral Diseases, National Institute of Allergy and Infectious Diseases, National Institutes of Health, Bethesda, MD 20892, USA.

Abstract

There is limited information about the impact of Zika virus (ZIKV) exposure *in utero* on the anti-ZIKV immune responses of offspring. We infected six rhesus macaque dams with ZIKV early or late in pregnancy and studied four of their offspring over the course of a year postpartum. Despite evidence of ZIKV exposure *in utero*, we observed no structural brain abnormalities in the offspring. We detected infant-derived ZIKV-specific IgA antibody responses and T cell memory responses during the first year postpartum in the two offspring born to dams infected with ZIKV early in pregnancy. Critically, although the infants had acquired some immunological memory of ZIKV, it was not sufficient to protect them against reinfection with ZIKV at one year postpartum. The four offspring re-exposed to ZIKV at one year postpartum all survived, but exhibited acute viremia and viral tropism to lymphoid tissues; three out of four re-exposed offspring exhibited spinal cord pathology. These data suggest that macaque infants born to dams infected with ZIKV during pregnancy remain susceptible to postnatal infection and consequent neuropathology.

Introduction

Zika virus (ZIKV) infections have now been reported in more than 80 countries, and outbreaks have occurred recently in new locations in Asia and Africa (1, 2). The number of documented ZIKV infections has declined in the Americas following the outbreak of 2015–2016, but the World Health Organization indicates that ZIKV could reemerge in the Americas, following the pattern of other epidemic-prone pathogens (1, 3). Previously unappreciated severe manifestations of congenital ZIKV infection including microcephaly and a spectrum of malformations called congenital Zika syndrome have become apparent in French Polynesia and Latin America during the last decade (4–7). In addition to fetal abnormalities that are evident during gestation, infants can also manifest congenital Zika syndrome postnatally in the presence or absence of overt clinical anomalies at birth (8–11). Few studies have longitudinally tracked infants and children after birth who are affected by congenital Zika syndrome (12, 13), and information about the postnatal impact of *in utero* ZIKV exposure is limited. This is because offspring from the peak of ZIKV activity in the Americas are currently no more than 5 years old. Also, this period has not yet been studied in nonhuman primates.

Nonhuman primates, particularly macaques, are the best described animal model of human ZIKV infection (14, 15). Macaques are a particularly relevant model for studying human congenital ZIKV infection because macaques and humans share similar hemomonochorial placentas, gestational stages, neuroanatomy, and immune system development (14–16). Thus far, ZIKV infection of pregnant macaques has sometimes resulted in severe fetal central nervous system (CNS) abnormalities but most often has been clinically unremarkable, consistent with the natural history of congenital ZIKV infection in humans (15). Macaques also are a useful model of postnatal development with the advantage of maturing three to four times faster than humans (15–17).

Gaining a better understanding of fetal and infant immune responses to ZIKV is particularly relevant because ZIKV vaccine trials and studies of passive antibody transfer to nonhuman primate adults have demonstrated that neutralizing antibody titers are close correlates of ZIKV immunity (14, 18–22). The role of antibodies during pregnancy and infancy is more complex, however. Delivery of neutralizing antibodies to infected pregnant animals has not prevented fetal ZIKV infection (23). Moreover, the timing and effectiveness of fetal immune responses remains a topic of controversy. Fetuses are known to have an immature immune system that is limited in its ability to respond to viruses as compared to adults (24–26). However, recent reports have indicated that fetal immune responses to foreign antigens may develop *in utero* with immune memory that lasts into childhood (25, 27–29).

We set out to address uncertainties about the early host immune response to ZIKV, once our longitudinal studies in pregnant macaques were completed and passive maternal immunity had waned in offspring. Here, we report the longitudinal analysis of macaque offspring born to ZIKV-infected rhesus macaque dams from gestation through an extended postnatal period. We evaluated whether the offspring born to ZIKV-infected mothers had acquired immunological memory to ZIKV that was sufficient to protect against ZIKV re-exposure. We monitored the offspring for ocular and brain structural alterations and overt neurological manifestations of congenital Zika virus syndrome during the first year of life. We characterized the ZIKV-specific antibody response to congenital ZIKV infection in offspring for one year after birth, a developmental stage similar to that of the oldest children born to ZIKV-infected mothers during the 2015–2016 epidemic.

Results

ZIKV kinetics and tropism in macaque dams and their fetuses during gestation

Data from the 2015–2016 epidemic suggested that ZIKV infection during early gestation was associated with increased prevalence of congenital Zika syndrome compared with exposure during late gestation (30). We began our study by infecting two cohorts of pregnant rhesus macaques with ZIKV early or late in gestation. The “early” cohort of dams was infected during the late first trimester (one animal, $E1_D$) or early second trimester (two animals, $E2_D$, $E3_D$) of pregnancy. The “late” cohort (three animals, $L1_D$, $L2_D$, $L3_D$) was infected early in the third trimester (Fig. 1). The dams were subcutaneously infected with 1×10^6 plaque-forming units (PFU) of ZIKV Paraiba/2015 strain, which has been associated with a high prevalence of infant microcephaly (31, 32). A control cohort (two animals, $M1_D$, $M2_D$) was mock-infected with saline alone. All ZIKV-infected dams developed short-term viremia with viral RNA peaking at 5.7–6.2 Log_{10} genome equivalents (GE)/ml (Fig. S1). We did not detect ZIKV RNA in the blood of any dam after 10 days post-infection. Conversely, we first detected ZIKV RNA in amniotic fluid of two dams ($E1_D$ and $E3_D$) more than 3 weeks after infection (Fig. 2). 23 days post-infection (d.p.i), we recovered 1.7 Log_{10} PFU/ml of infectious ZIKV from the amniotic fluid of dam $E3_D$. The amniotic fluid contained 7.3 Log_{10} GE/ml of ZIKV RNA, a log higher than we found in the blood of infected dams. We also detected ZIKV RNA in the amniotic fluid of $E1_D$ at 79 d.p.i. indicating that its fetus, $E1_I$, was exposed to ZIKV during gestation, weeks after ZIKV was cleared from the blood of dam $E1_D$. To investigate prenatal viral tissue tropism and pathology, one maternal-fetal

pair from each cohort ($E1_D$–$E1_I$ and $L1_D$–$L1_I$) was sacrificed at the time of delivery. Using droplet digital PCR (ddPCR) for increased sensitivity, we found no ZIKV RNA in the 23 tissues we sampled from $E1_D$ and $E1_I$, (Fig. S2) despite the presence of ZIKV RNA in the amniotic fluid 4 weeks before necropsy. We detected ZIKV RNA in the inguinal lymph node and spleen of $L1_D$, but detected none in the tissues of fetus $L1_I$.

No observed abnormalities in fetal macaques after ZIKV exposure *in utero*

We detected no abnormalities in the rate of biparietal diameter growth (the standardized measurement of the transverse distance across the fetal skull) for any of the fetuses despite *in utero* exposure to ZIKV. Biparietal diameters measured by serial ultrasonography during gestation remained within two standard deviations of predicted growth means for rhesus macaques (Fig. S3)(33). Brain MRI performed on each of the fetuses during the third trimester showed no gross abnormalities (Fig. S4A). Fetal intracranial volume (ICV) measurements did not show (P=0.3297) differences between two control animals and six animals born to infected dams, all imaged between 17 and 20 weeks of gestational age (Fig. S4B). Further, no abnormalities were detected by histological evaluation of brain tissues collected from the maternal-fetal pairs sacrificed at the time of delivery (Tables S1, S2).

Longitudinal analysis of prenatal and postnatal ZIKV-specific antibody responses

All infected dams mounted ZIKV-specific neutralizing antibody responses (Fig. 2). The neutralizing antibodies were detectable in the maternal circulation at 7 d.p.i. and 5 of the 6 dams reached a peak neutralizing antibody titer in the plaque reduction neutralization test ($PRNT_{50}$) of 2–8×10^3 by 42 d.p.i. The dam with the highest viral RNA in its amniotic fluid, $E3_D$, produced a $PRNT_{50}$ measurement that was a full log higher (4×10^4) than that for the other dams (Fig. 2). We detected this highest neutralizing antibody titer at 51 d.p.i., 9 days after we detected viral RNA in the amniotic fluid of $E3_D$. Following delivery, neutralizing antibody titers gradually decreased in each of the surviving dams ($E2_D$, $E3_D$, $L2_D$, $L3_D$), but remained detectable for as long as they were measured (at least 100 d.p.i.).

We used a surface plasmon resonance (SPR) assay to determine the isotypes of the antibodies specific for the ZIKV envelope protein and nonstructural 1 (NS1) protein. We first demonstrated the specificity of the assay for detection of rhesus macaque antibody isotypes (Fig. S5). As expected in a primary immune response, maternal IgM was highest at the earliest time-points we tested following inoculation with ZIKV (Fig. 3A, Fig. S6A). We detected envelope protein-specific IgM above background in dam $E1_D$ until 42 d.p.i., in $E2_D$, $E3_D$ and $L1_D$ until 23 d.p.i, and in $L3_D$ only until 7 d.p.i. IgA antibodies were also readily detectable in the blood of 5 of 6 ZIKV-infected dams by 7 d.p.i. and peaked around 21 d.p.i (Fig. 3A). Envelope-specific IgA was detectable at every time-point tested after 7 d.p.i. in all dams (Fig. 3A). IgG was the predominant isotype in the circulation from 7 d.p.i. onwards in all dams (Fig. 3A). Envelope-specific IgG generally peaked around 45 d.p.i., and like IgA, persisted in all surviving animals near peak amounts until 79 d.p.i.

Due to the longitudinal nature of the study, we were able to carry out a new investigation of the ZIKV-specific neutralizing antibodies in the four surviving offspring a year after birth. The four infant macaques were breastfed for approximately 6 months after birth.

About two weeks after birth, total circulating neutralizing antibody titers in three of the four infants were found to be similar to those of their respective dams (Fig. 2). Unlike the other three offspring, $L3_I$ had lower neutralizing antibody titers than its dam for several weeks after delivery before reaching the same amount as in maternal blood by 6 weeks postpartum. The neutralizing antibody titers of all four infants waned after birth (Fig. 2). $PRNT_{50}$ measurements remained above the limit of detection for 140 days after birth (231 d.p.i.) for $E2_I$, 185 days after birth (288 d.p.i.) for $E3_I$, 60 days after birth (107 d.p.i.) for $L2_I$, and 136 days after birth (181 d.p.i.) for $L3_I$ (Fig. 2)

Amongst antibodies against envelope protein or NS1 protein, we detected no IgM in the circulation of the four infants ($E2_I$, $E3_I$, $L2_I$, $L3_I$) from birth until one year of age (Fig. 3B, Fig. S6B). In contrast, about 2–7% of the envelope-specific or NS1-specific neutralizing antibodies in the infant circulation had an IgA isotype (Fig. S5B). The percentage of IgA antibodies generally increased in the infants, but absolute amounts waned in the weeks after birth, remaining above background in infant $E2_I$ for 31 days after birth (122 d.p.i.), infant $E3_I$ for 78 days after birth (181 d.p.i.), infant $L2_I$ for 12 days after birth (59 d.p.i.), and infant $L3_I$ for 42 days after birth (87 d.p.i.) (Fig. 3B, Fig. S6B). Greater than 90% of the infants' circulating envelope-specific or NS1-specific neutralizing antibodies had an IgG isotype throughout the time-points we tested after birth (Fig. 3B, Fig. S6B). IgG also waned but remained detectable throughout the SPR assay testing period in the circulation of infants $E2_I$, $E3_I$, and $L3_I$. In contrast, IgG in the circulation of infant $L2_I$ fell below the limit of detection by 102 days after birth (147 d.p.i.).

No ocular or structural brain manifestations of congenital Zika syndrome were observed for one year postpartum

Offspring of mothers who were infected with ZIKV during pregnancy can develop congenital Zika syndrome in the absence of overt clinical anomalies at birth (8). As a result, we observed macaque infants $E2_I$, $E3_I$, $L2_I$, and $L3_I$ for developmental abnormalities during their first year of life, which is considered similar to the first three years of human development (17). We did not detect ZIKV RNA during regular sampling of the blood (Fig. 2) or the cerebrospinal fluid (CSF; Table S3) of infants $E2_I$, $E3_I$, $L2_I$, and $L3_I$ beginning two weeks after birth until one year of age. We conducted a subset of Brazelton exam tests to quantitatively score behavioral development two weeks and four weeks postpartum. The Brazelton exam is designed to assess a variety of attentional, neuromotor, and temperamental responses and characteristics that mature during the first month of life in nonhuman primates. The exam included 24 tests (scored from 0–2, lowest to highest), a subset of those that were previously validated for rhesus macaques to assess behavioral clusters such as orientation and motor maturity (34). At two weeks postpartum, the scores of $E2_I$, $E3_I$, $L2_I$, and $L3_I$ averaged 0.80, whereas the scores of $M2_I$ averaged 0.83 (Data File S1). At four weeks postpartum, the scores for $E2_I$, $E3_I$, $L2_I$, and $L3_I$ averaged 1.05, whereas the scores for $M2_I$ averaged 1.07 (Data File S1).

Approximately six months after delivery, the brain of each infant was analyzed by MRI and was found to be grossly normal with no evidence of intracranial calcifications, ventricular abnormalities or gliotic foci (Fig. S4C). Intracranial brain volumes of the infants were not

compared because the infants were imaged at slightly different ages (from 7–9 months). We conducted ophthalmic exams three times (once when the offspring were about 6 months old, once two weeks before ZIKV reinfection at about 14 months old, and once after the reinfection). The only abnormal finding on any exam was an avascular area on the macula during the 6-month exam of $E3_I$ (Table S4). However, this was not noticed on follow-up exams. The rest of the exams were normal, and none of the animals exhibited any gross indications of vision impairment based on the physical exams. Histopathological examination of eye tissue after necropsies at delivery (Table S2) and after the reinfection studies (Data File S2) also revealed no abnormalities. The offspring were clinically observed over the entire length of the study by a trained veterinarian. Physical exams were done routinely when the animals were sedated. The animals were also qualitatively observed daily for appetite, overt neurological abnormalities, and activity/lethargy. No abnormalities were noted from these exams throughout the study period.

Development of immune memory does not protect against ZIKV reinfection

Once passive immunity acquired from the dams had completely waned prior to one year after birth, we sought to determine if the infants had mounted their own anti-ZIKV immune responses. Based on our data and previous nonhuman primate studies that have reported ZIKV transmission from dams to fetuses (14, 15, 35), we expected all of our offspring to have been exposed to ZIKV. Specifically, we investigated whether the offspring had generated ZIKV-specific immunological memory and whether this memory was sufficient to protect them against a subsequent postnatal ZIKV infection. To do this, we infected two cohorts of animals with ZIKV (Fig. 4). The first cohort was comprised of animals born to dams that were not infected with ZIKV during pregnancy. This cohort included 15-month-old $M2_I$ and two additional two-year-old animals (C1 and C2). The second cohort was comprised of the remaining 13–15-month-old offspring ($E2_I$, $E3_I$, $L2_I$, $L3_I$) born to dams that were infected with ZIKV while pregnant. We infected all seven animals with the same strain and dose of ZIKV used for the primary infection. One day after infection, we detected similar amounts of ZIKV RNA in the blood of all seven animals (Fig. 5A). ZIKV RNA ranged from 5.4–6.2 Log_{10} GE/ml in the first cohort and 5.5–6.6 Log_{10} GE/ml in the second cohort. We detected ZIKV RNA in the CSF of animals from both cohorts ($M2_I$, $E3_I$, and $L2_I$) at 2 d.p.i. Amounts of circulating ZIKV RNA in both cohorts at 3 d.p.i, were similar to the amounts found in the dams three days after they were infected at the start of the study (Fig. S1). We began to detect a circulating ZIKV-specific neutralizing antibody response in animals of both cohorts at 5 d.p.i. (Fig. 5B). All 7 animals mounted ZIKV-specific antibody responses with similar kinetics and magnitude (Fig. 5B). Two weeks after reinfection, ZIKV tissue tropism was similar across the two cohorts (Fig. 5C).

Because we expected that the offspring in the second cohort had been exposed to ZIKV, we wished to confirm that the second cohort had acquired no memory T cells specific for ZIKV. We tested peripheral blood mononuclear cells (PBMCs) collected from infants $M2_I$, $E2_I$, $E3_I$, $L2_I$, and $L3_I$ more than a year after birth and one month prior to reinfection. We also tested PBMCs collected from dam $E2_D$ at 23 d.p.i. and from animals C1 and C2 before they were initially infected. After stimulating the cells for 6 hours with overlapping ZIKV envelope and NS1 peptides, we looked for memory $CD4^+$ and $CD8^+$ T cells producing the

anti-viral effector cytokines TNFα or IFNγ (Fig. S7). Animals C1, C2, and $M2_I$ had never been exposed to ZIKV, and they did not have any ZIKV-specific memory T cell populations (Fig. 5D). Dam $E2_D$, which had been subcutaneously inoculated as an adult, had both ZIKV-specific $CD4^+$ and $CD8^+$ memory T cells producing both TNFα and IFNγ (Fig. 5D). The two offspring of dams infected with ZIKV early in pregnancy had some ZIKV-specific memory T cells that responded to the peptides. Infant $E2_I$ had $CD8^+$ memory T cells that produced TNFα (Fig. 5D). Infant $E3_I$ had $CD8^+$ memory T cells that produced IFNγ and TNFα (Fig. 5D). Conversely, we did not detect ZIKV-specific memory T cells in the two offspring of the dams infected with ZIKV later in pregnancy.

CNS pathology was observed in offspring born to ZIKV-infected dams after ZIKV reinfection

Postmortem CNS tissues from the first cohort ($M2_I$ C1, C2; no prior exposure to ZIKV) and the second cohort ($E2_I$, $E3_I$, $L2_I$, $L3_I$, born to dams infected with ZIKV during pregnancy) were processed, coronally sectioned, and evaluated for histopathology. We identified Wallerian degeneration (axon injury that results in no distal viability) in 3 of 4 spinal cords ($E2_I$, $E3_I$, $L3_I$) from the second cohort (Table S5; Fig. 5E). In contrast, Wallerian degeneration was not observed in CNS tissues in the first cohort (Fig. 5F). There was Wallerian degeneration in multiple cervical, thoracic and lumbar segments of the spinal cords characterized by multifocal, mild axonal swelling with infiltrating macrophages and digestion chambers in the cytoplasm of Schwann cells. Digestion chambers are associated with myelin destruction after the start of Wallerian degeneration (36). The acute Wallerian degeneration we observed at this time-point was not extensive enough to be noticed clinically. We did not detect ZIKV in the spinal cord lesions or locate an initial point of injury above the axonal damage. Infant $E3_I$ had a focally extensive lesion in the lumbar spinal cord consisting of marked microgliosis of gitter cells with phagocytized debris and multifocal axonal swelling and necrosis (Fig. S8A). Glial fibrillary acidic protein (GFAP), an astrocyte marker, showed a marked increase in astrocytic processes and subsequent glial scars (Fig. S8B). Ionizing calcium binding adaptor molecule 1 (Iba1), a microglial marker (Fig. S8C), and CD68, a macrophage marker, showed increased expression in the lesion found in the lumbar spinal cord segment of infant $E3_I$. In situ hybridization with a ZIKV antisense oligonucleotide probe targeting genomic RNA (Fig. S8D, E) and a ZIKV sense oligonucleotide probe targeting replicative RNA intermediates was negative in this lesion (Fig. S8F).

After observing spinal cord pathology only in the cohort that was previously exposed to ZIKV, we used a sensitive and quantitative ZIKV reporter virus particle assay (37, 38) to investigate whether this cohort possessed infection-enhancing antibodies that contributed to the pathology. No antibody-dependent enhancement (Fig. S9A) or neutralization (Fig. S9B) of ZIKV infection was detected in blood collected from infants in both cohorts prior to ZIKV infection. Two weeks post-infection, antibody-dependent enhancement (Fig. S9C) and ZIKV-specific neutralization (Fig. S9D) were detected in all animals as expected, and the magnitude of the response was not higher in the *in utero*-ZIKV exposed cohort compared to the naïve cohort (Fig. S9E–F).

We also identified multifocal mineralization of unknown etiology within the brains of six of the seven animals in the ZIKV reinfection study (Table S5; Fig. S10A). Animal C2 did not have evidence of mineralization (Fig. S10B), whereas four animals (C1, $M2_I$, $E3_I$ and $L2_I$) had minimal deposits. Infants $E2_I$ and $L3_I$ had moderate and mild numbers of mineralized deposits, respectively (Table S5). The mineralization was located predominantly within the globus pallidus of the macaque brain, but extended to other regions within the basal ganglia. Mineralized lesions were often perivascular but could be found randomly in the CNS without evidence of underlying vasculature; there was no accompanying inflammatory reaction or gliosis. The mineralization was often arranged in single to multiple grape-like basophilic clusters frequently showing a concentric layered or lamellar ring. Mineralized lesions appeared basophilic and granular after staining with hematoxylin and eosin. They stained positive with periodic acid-Schiff stain (Fig. S10C) and von Kossa stain and negative with Prussian blue iron stain. Iba1 immunohistochemistry highlighted microglial processes surrounding areas of mineralization (Fig. S10D); there was no increase in GFAP expression in these lesions (Fig. S10E).

Discussion

There is currently a shortage of data about the postpartum ZIKV-specific host immune response after ZIKV infection *in utero*. We designed a nonhuman primate study focused on the ZIKV-specific antibody response because of its importance for protection against infection and vaccine development (14). We serially investigated the kinetics of the ZIKV-specific antibody response in the circulation of 4 macaque infants born to ZIKV-infected dams. Similar ZIKV-specific neutralizing antibody titers in the infants and their mothers could mean that the neutralizing antibodies in the infant circulation were primarily maternally-derived IgG that had passed through the placenta before birth. Comparison of ZIKV-specific neutralizing antibody titers in the infants and their mothers indicated that the neutralizing antibodies in the infant circulation were maternally derived IgG. These data align with historical findings in macaques and humans that serum IgG concentrations in infants are within 10–15% of maternal concentrations at birth(39). In our study, detectable ZIKV-specific neutralizing antibodies in the infant circulation gradually waned after birth. We would expect this to happen in the absence of ongoing or new ZIKV infection in the infants, but it was also possible that the infants' immature immune system was incapable of generating its own neutralizing antibody responses or that the infants displayed tolerance to viral antigens which they were exposed to during gestation.

To further characterize the origin and function of ZIKV-specific antibody responses, we identified their isotype. These data are important because they provide evidence that the infants produced their own anti-ZIKV serum IgA and possibly harbored ZIKV postnatally. In support of this, historical data show that macaque and human newborns are born with low to undetectable serum IgA in the absence of infection(40). The macaque infants received secretory IgA-rich breastmilk for about 6 months after birth, but this maternally-derived IgA did not contribute to serum titers. Antibodies in the breastmilk are not believed to pass through the intestinal epithelium and into the circulation of humans and nonhuman primates (41). In this context, it is important to note that although the infant ZIKV-specific IgA titers were readily detectable, the titers did decrease after the first month of life. This

suggested that perhaps the newborns re-encountered ZIKV during delivery or were forced to control intrauterine-acquired ZIKV independent of the maternal immune system soon after delivery. Compared to mucosal IgA, the immunological function of serum IgA is relatively unexplored (42). Early and sustained elevated serum IgA titers suggest that the role of serum IgA in the anti-ZIKV immune response should be a topic for future studies. This observation also supports recent studies that identified acute IgA titers after ZIKV infection in humans as a possible diagnostic target (43, 44).

Once the macaque offspring reached 13–15 months of age (~3–4 years of human maturation), we re-exposed them to ZIKV by inoculating them subcutaneously with the same strain and dose (1×10^6 PFU) of ZIKV that we had administered to the dams at the start of the study. We purposely waited to do this until all maternal passive immunity had waned in the offspring. A recent pilot study showed that 2 macaques born to ZIKV-infected dams exhibited more controlled viremia after re-exposure compared to once-infected adults from other studies(45). The dams received primary ZIKV infection late during gestation, and the offspring were re-exposed 5 months after birth when ZIKV-specific antibodies, likely derived from the dams, were still detected in the serum (45). With our study, we were able to further characterize the ZIKV-specific immune response of offspring *in utero* and after birth by determining whether they were immunologically protected against reinfection in the absence of maternal passive immunity and using an age-matched control group.

From the results of the ZIKV reinfection study, we drew several conclusions with epidemiological and immunological implications. First, the data demonstrate that *in utero* exposure to ZIKV does not confer immunological protection against a subsequent ZIKV infection after birth. Given the similarity of the macaque model of congenital ZIKV infection to human congenital ZIKV infection, it is possible that the same may be true for asymptomatic human offspring born to ZIKV-infected mothers. Although adults and many children do not experience severe disease after ZIKV infection, a recent study of infant macaques demonstrated that ZIKV infection shortly after birth can induce severe CNS pathology(46). Second, the data provide more evidence of an immune response mounted by the infants against ZIKV. The two offspring born to ZIKV-infected mothers infected early in gestation were capable of mounting their own ZIKV-specific memory T cell responses. It is not possible from our data to know for certain whether this immune response was initiated *in utero* or after birth, but recent studies indicate that immunological memory can begin to develop *in utero* (25, 27–29). Third, the appearance of Wallerian degeneration we found in the spinal cords of the *in utero* exposed cohort after the reinfection study indicated that it was acute and not chronic pathology (36). The fact that we found the Wallerian degeneration only in the previously exposed cohort suggested that prior *in utero* ZIKV exposure promoted spinal cord pathology in the reinfected offspring. It is not clear from our data why the spinal cord pathology was limited to the previously exposed cohort. Because of the small macaque numbers in our study, this is a critical area for further investigation. It is also not clear from our data exactly why the offspring born to ZIKV-infected mothers were not protected against reinfection even though ZIKV exposure during adulthood confers immunological protection(47, 48). We hypothesize that the compromised antiviral immune response of the fetus and the immature immune system of the neonate both may contribute to this finding despite evidence that the same animals were capable of developing a ZIKV-specific memory

T cell response in the first year of life. In a recent pilot study of 2 macaque neonates re-exposed 5 months postpartum to ZIKV, the moderate protection observed could be due to lingering maternal transfer of antibodies. Those antibodies were absent by the time we re-exposed our offspring to ZIKV. Lastly, it is worth noting that the brain histopathology analysis from the ZIKV reinfection study supported a previous observation that idiopathic mineralization occurs frequently in nonhuman primate brains(49). Brain mineralization in nonhuman primates is not as reliable a ZIKV-specific injury as it may be in humans infected with ZIKV.

There are several limitations to our study that are important to note. The biggest constraint in drawing conclusions from our data is the small number of nonhuman primates in our study. In particular, the small number of mock-infected control animals restricted our ability to establish whether there was a consistent background amount of pathology in the study animals and our ability to draw powerful statistical comparisons between some study cohorts (e.g. with the Brazelton exam). Also, despite finding evidence that macaque infants $E2_I$, $E3_I$, $L2_I$, and $L3_I$ each produced a ZIKV-specific immune response, we did not find evidence that the offspring in the reinfection study had a prior productive infection. Thus, the conclusions of this study may or may not be relevant to human infants who harbored a productive ZIKV infection *in utero*.

Because there is currently limited available information about the impact of congenital and postnatal ZIKV infection during the postnatal period in humans, it is essential that we use the best available animal model to address this knowledge gap. Collectively, our data from pregnant macaque dams infected with ZIKV and their offspring provide insights and focus new questions about the ZIKV-specific host immune response during gestation and in the first year of life, a critical period as we seek to design therapies and ultimately prevent ZIKV-related disease.

Materials and Methods

Study design

The initial objective of this study was to longitudinally investigate pathogenesis and immunological correlates of congenital Zika syndrome in macaques postpartum after exposure to ZIKV *in utero*. We mock-infected or ZIKV-infected pregnant rhesus macaque dams and then investigated the ZIKV-specific host immune responses of asymptomatic offspring born to dams infected with ZIKV early or late in pregnancy. We determined whether the immune responses of the macaque offspring were sufficient to protect against ZIKV reinfection a year after birth. We assessed prenatal and postnatal ZIKV kinetics and tissue tropism in dams and offspring using qPCR and ddPCR, and dam and infant humoral immune responses using a $PRNT_{50}$ assay, surface plasmon resonance, flow cytometry, and an antibody-dependent enhancement assay. Histopathology was assessed in two dam/infant pairs at delivery and also in the remaining offspring two weeks after reinfection with ZIKV. We looked for any developmental abnormalities in offspring *in utero* and up to 13–15 months postpartum after ZIKV infection of pregnant dams using prenatal and postnatal MRI, fetal ultrasound imaging, ophthalmic exams, regular physical exams, and daily clinical observations.

The dams were randomly chosen from a breeding colony and randomly assigned to experimental groups at the start of the study. Investigators were blinded to the identity of the groups for assessment of outcomes. We began the study with 9 dams and maximized the number in each group (n=3). Samples and assays were run in duplicate or triplicate when possible after consideration of ethical animal sampling guidelines. Samples or data points were excluded only in the case of a technical equipment error or human error. One maternal/fetal pair was removed from the mock-infected group after a miscarriage. No other animals were excluded from the study.

This nonhuman primate study was conducted with the approval and oversight of the National Institute of Allergy and Infectious Diseases Division of Intramural Research Animal Care and Use Committee as part of the National Institutes of Health Intramural Research Program (protocol LID 37). Rhesus macaques (*Macacca mulatta*) were housed and sustained in accordance with standards established by the Association for Assessment and Accreditation of Laboratory Animal Care (AAALAC). 8 female Indian-origin rhesus macaques seronegative for dengue virus and West Nile virus served as dams. Sexes of the offspring followed longitudinally were as follows: $M2_I$ and $E3_I$ were females, and $E2_I$, $L2_I$, and $L3_I$ were males. The 2 additional control animals for the ZIKV reinfection study (C1 and C2) were also seronegative for dengue virus and West Nile virus. They were both 2-year-old females. All animals were cared for at the National Institutes of Health Animal Center.

Characteristics of the Zika virus strain

The ZIKV-Paraiba/2015 strain was originally isolated in the state of Paraiba, Brazil in 2015 from a serum sample of an acutely infected patient and was provided by Pedro Vasconcelos, Instituto Evandro Chagas, Brazil. The virus isolate was terminally diluted and passaged twice in Vero cells to generate a working stock. Virus titer ($\log_{10}$ PFU/ml) was determined by plaque assay in Vero cells. Vero cells were cultured in OptiPro SFM medium (Life Technologies) supplemented with 4 mM L-glutamine (Life Technologies) and kept at 37°C (5% CO_2 and 80% relative humidity) until confluent. To prepare the inoculum, the working stock of ZIKV-Paraiba/2015 was diluted in 2X L-15 medium (Lonza) and water for injection to yield an infectious titer of 6.0 $\log_{10}$ PFU/ml in 1X L-15 medium. The inoculum was kept on ice before administration and used within 3 hours. 0.5ml of inoculum was subcutaneously injected into the right shoulder and the left shoulder for a total injection volume of 1.0ml. Stability of virus titer was confirmed by back-titration of the inoculum by plaque assay both 0 and 3 hours after preparation.

Fluid sample collection

Animals were sedated with 100mg/ml Ketamine between 10mg/kg and 20mg/kg. Blood was collected from the femoral vein and CSF was collected percutaneously via the cisterna magna using aseptic technique each time the animals were sedated between birth and the reinfection study (every two weeks after delivery for eight weeks and then every four weeks). During the reinfection study, blood was collected on all days −14, 1–5, 7, 10, 12 and at necropsy. CSF was collected on days −14, 3, 7, and at necropsy. Amniotic fluid was collected from the dam aseptically. Ultrasonography was utilized to identify the appropriate

area to obtain the amniotic fluid but avoid the fetus and placenta. A 22 X 1.5 inch needle was inserted into the uterus with ultrasound guidance, 0.3ml of amniotic fluid was collected. Amniotic fluid was collected weekly starting seven days after the inoculation with the virus.

Clinical observations

Animals were administered an entrance physical examination prior to assignment to the study. Animals were observed before pre-dose and approximately 2, 4, and 6 hours post-dose on days of ZIKV inoculation and at least twice daily thereafter for signs of poor health or abnormal behavior. Special attention was directed to any signs of neurological symptoms, hemorrhagic disease, or dermal effects especially at the sites of inoculation. During post-partum and infancy periods, nursing and mother-infant interactions were closely observed. Additional physical examinations were done each time cerebrospinal fluid was collected, 14 days before reinfection, and 2, 7, and 14 days after reinfection. Animals were also qualitatively monitored daily for appetite, overt neurological abnormalities, and activity/lethargy. Full physical exams included recording weight, rectal temperature, heart rate, and respiratory rate each time animals were sedated.

Brazelton exam assessment

In postnatal weeks 2 and 4, prior to sedation for labs, the infants were given a battery of tests designed to assess neonatal neurobehavioral development. The test battery was a subset of those tests derived from the Brazelton Neonatal Assessment Scale, modified for rhesus monkeys(34). All test items listed by cluster in Data File S1 were scored on a 2-point scale with 2 being the best score. All tests were conducted by a single experienced research veterinarian, Richard Herbert, D.V.M., at the same time of day to minimize inter-tester and temporal variations.

Ophthalmic exam

Examinations were performed at 6 months postpartum, 2 weeks before the reinfection study, and 2 weeks after the reinfection study. Animals were anesthetized with ketamine (10mg/kg intramuscularly), and their eyes were dilated with a mydriatic agent prior to examination. An indirect ophthalmoscope was used to visualize the cornea, pupil, lens, and retina. Ambient light was reduced for 3–4 hours after the exam.

ZIKV detection in fluids by qPCR

Viral RNA was extracted from nonhuman primate-derived serum, plasma, CSF, and amniotic fluid using the EZ1 Virus mini kit v2.0 (Qiagen). cDNA was synthesized with the SuperScript III First-Strand Synthesis System (Life Technologies) using random hexamer primers. Absolute quantification of virus genome equivalents (Log_{10} GE/mL) was determined by real-time PCR using a TaqMan probe (Integrated DNA Technologies) targeting the ZIKV envelope protein. The limit of detection was 3.2 Log_{10} GE/ml.

ZIKV detection in tissues by ddPCR

Total RNA was extracted from RNA*later* (Invitrogen, Hampton, NH, USA) preserved tissues collected at necropsy using the RNeasy Plus Universal Mini kit (Qiagen, Germantown, MD,

USA) according to the manufacturer's protocol. Flash frozen tissue samples were used in select instances instead. The upper and lower left hemisphere of the brain was sampled by punch biopsy. Prior to extraction, tissues were suspended in QIAzol Lysis Reagent (Qiagen) and mechanically homogenized on the TissueLyser (Qiagen) using stainless steel beads. The NanoDrop 8000 Spectrophotometer (Thermo Scientific, Waltham, MA, USA) was used to quantify RNA concentrations prior to reverse transcription using the iScript Advanced cDNA Synthesis Kit for RT-qPCR (Bio-Rad, Hercules, CA, USA). The QX200 AutoDG Droplet Digital PCR System (Bio-Rad, Hercules, CA, USA) was used to detect and quantify ZIKV RNA using a custom designed ddPCR Copy Number Variation Assay (Bio-Rad, Hercules, CA, USA) targeted against the envelope (E) gene region: forward (5'-CCGCTGCCCAACACAAG-3'), reverse (5'-CCACTAACGTTCTTTTGCAGACAT-3'), probe FAM (5'-CTACCTTGACAAGCAATCAGACACT-3'). 96 well plates were prepared with ddPCR Supermix for Probes (No dUTP) and the aforementioned custom primer/probe set according to the manufacturer's instructions (Bio-Rad, Hercules, CA, USA), and samples were added in technical replicates with up to 1000 ng cDNA per well. The QX200 Automated Droplet Generator (Bio-Rad, Hercules, CA, USA) provided microdroplet generation and plates were sealed with the PX1 PCR Plate Sealer (Bio-Rad, Hercules, CA, USA) before proceeding with PCR on the C1000 Touch Thermal Cycler (Bio-Rad, Hercules, CA, USA) using a 55°C annealing/extension temperature. Plates were read on the QX200 Droplet Reader (Bio-Rad, Hercules, CA, USA) to determine the number of droplets containing the ZIKV target sequence. Manufacturer provided QuantaSoft Software (Bio-Rad, Hercules, CA, USA) was used to analyze the data and quantify ZIKV copies per well, which was then normalized to the RNA concentration input during reverse transcription. The limit of detection was 1.4 ZIKV copies per well.

Plaque assay for titration of infectious virus

Fluid samples were tested for the presence of infectious virus by plaque assay in Vero cells. The assay was carried out by serially diluting the samples (10-fold) beginning at 1:10 in a round-bottom 96-well plate (Thermo Scientific) containing cold OptiMEM GlutaMAX medium (Life Technologies). Then 24-well plates (Corning) containing Vero cell monolayers were inoculated and subsequently incubated at 37°C with occasional rocking for 1 hr. After incubation, cells were overlaid using OptiMEM GlutaMAX (Life Technologies) supplemented with 1% methylcellulose (Sigma), 2% fetal bovine serum (FBS) (HyClone), 20 ug/mL ciprofloxicin (Sigma), and 2.5 ug/mL amphotericin B (Quality Biologicals) and incubated for 3 days at 37°C. Plaques were visualized by immunoperoxidase staining. Briefly, cell monolayers were washed twice with phosphate-buffered saline (PBS), fixed in 80% methanol for 10 min and blocked with antibody buffer (5% nonfat milk in PBS) for 10 min, all at room temperature. A pan-flavivirus (4G2) monoclonal antibody was diluted in antibody buffer and added to each well followed by a 2 hr incubation at 37°C. Primary antibody was removed and the cell monolayers were washed twice with antibody buffer. Peroxidase-labeled goat-anti-mouse IgG (KPL) was diluted in antibody buffer and added to each well, followed by a 2-hr incubation at 37°C. Secondary antibody was removed, and the wells were washed twice with PBS. True-Blue™ peroxidase substrate (3,3',5,5'-Tetramethylbenzidine)(KPL) was added to each well and plaques were counted and titers ($\log_{10}$ PFU/mL) were calculated for each sample.

Plaque-reduction neutralization test ($PRNT_{50}$)

Briefly, test sera were heat inactivated (56°C for 30 min) and serial four-fold dilutions beginning at 1:5 were made in OptiMEM GlutaMAX supplemented with 0.5% human serum albumin (Grifols), 2% FBS and 50 ug/ml gentamicin (Life Technologies). The ZIKV Paraiba/2015 virus, diluted to a final concentration of approximately 580 PFU/ml in the same diluent, was added to equal volumes of the diluted serum and incubated at 37°C for 30 min. Cell culture medium was removed from confluent monolayer cultures of Vero cells on 24- well plates and 100 ul of virus/serum mixture was transferred onto duplicate cell monolayers. Cell monolayers were incubated for 60 min at 37°C and overlaid with methylcellulose medium as described above. Samples were incubated at 37°C for three days after which plaques were visualized by immunoperoxidase staining as described above, and a 50% plaque-reduction neutralization titer was calculated. 1:5 was the limit of detection because 1:5 was the initial dilution used.

Tissue histology and pathology

Tissues were fixed in 10% Neutral Buffered Formalin for x2 changes for a minimum of 7 days. Tissues were then portioned for both cryo- and paraffin-embedded sectioning. Tissues to be used for paraffin embedded sectioning were placed in cassettes and processed with a Sakura VIP-7 Tissue Tek on a 12 h automated schedule using a graded series of ethanol, xylene, and Ultraffin. Prior to fixation, the brain was coronally sectioned into 5 slices. Slices were numbered from 1 to 5 with 1 being the most anterior slice and 5 being the most posterior. Embedded tissues were coronally sectioned at 5 μm and dried overnight at 42°C prior to staining with hematoxylin and eosin (H&E), periodic acid-Schiff (PAS), von Kossa, Prussian blue, *in situ* hybridization (ISH) or immunohistochemistry (IHC). 10 coronal sections of brain tissue were evaluated per animal. Every 10^{th} spinal cord section was evaluated. Tissues to be used for cryosectioning were cryoprotected by overnight incubation in 30% sucrose/phosphate buffered saline and then frozen in Tissue Tek OCT at −20°C. Tissues were sectioned at 10μm and dried for 1hr at RT on Superfrost Plus slides prior to storage at −20°C. Detection of ZIKV RNA by ISH was performed using the RNAscope 2.5 VS assay (Advanced Cell Diagnostics Inc.) on the Ventana Discovery ULTRA as previously described(50) and in accordance with the manufacturer's instructions. Briefly, tissue sections were deparaffinized and pretreated with heat and protease before hybridization with V-ZIKA-pp-02 probe for ZIKV (ACDBio). Peptidylprolyl isomerase B (Ppib) and the bacterial gene, *dapB*, were used as positive and negative controls, respectively. For IHC, sections were processed and imaged as previously described(51). Antibodies against GFAP (1:3000, Dako), ZIKA NS5 (1:3000, Aves Labs), and NeuN (1:2500, abcam) or Sox2 (1:750, abcam) or Iba1 (1:250, Dako) or active Caspase 3 (1:250, Promega) were used at the indicated concentrations. Secondary antibodies (goat anti-chicken AF488, 1:500 and donkey anti-rabbit AF594, 1:500) were used to label specific primaries. For transmitted light staining, pan-flavivirus-4G2 (1:100, EMD Millipore) primary and goat anti-rabbit HRP (1:500) secondary were used and visualized via a 3,3'Diaminobenzidine chromogen (abcam).

Fetal and neonatal magnetic resonance imaging

Fetal macaques were sedated via an intramuscular injection of 10 mg/kg of ketamine. They were intubated and maintained under anesthesia with 1–2% isoflurane gas throughout the scanning. In situ imaging was done with a 3T Philips Achieva TX scanner using a 6-channel cardiac receive coil. Sequences: MultiVane (PROPELLER): FOV = 18 cm^2, res = 0.75mm^3, TR/TE = 4000/150 ms, ~73 contiguous slices, SENSE (y) = 2, fat saturation, NSA = 5, correction for rigid body motion between blades, scan time 9:55. 3D T2 FLAIR: FOV = 23×20 cm^2, y-SENSE = 2.6, slices = 46, res = 0.5×0.5×1mm^3, TR/TE = 4800/347 ms, TI = 1650 ms, T2Prep = 4´125 ms, NSA = 5, scan time: 10:30. 3D MPRAGE: TR/TE = 13.4/6.6 ms, TI: 837 ms, FOV = 16–17 cm, Flip angle: 8°, Res: 0.5×0.5×1 mm3, 69 slices, NSA = 4, Scan time: 5:19. All post-processing was carried out in Matlab. Intracranial volume (ICV) was determined from the MultiVane sequence images using a semi-automated segmentation method. Manual ROIs were drawn in the skull bone to separate the brain from surrounding fetal and abdominal tissue. This was followed by automated segmentation to remove remaining unwanted voxels leaving CSF, GM and white matter.

Neonatal macaques were scanned with a 3T Philips Achieva TX scanner using a 32-channel head coil. Sequences: 3D T2-TSE: FOV = 16×16 cm2, res: 1 mm3, y-SENSE = 2, z-SENSE =2.5, TR/TE = 2500/244 ms, NSA = 4, scan time: 2:53. 3D T2-w FLAIR: FOV = 16×16 cm2, res: 1 mm3, y-SENSE = 3, z-SENSE =2, TR/TE = 2500/290 ms, TI = 1650 ms, NSA = 8, scan time: 5:50. 3D MPRAGE (T1-w): FOV = 16×16 cm2, res: 0.5×0.7×1mm3, flip = 8°, y-SENSE = 2, z-SENSE =2, TR/TE = 13.4/6.6 ms, TI/TR(shot) = 837/1670 ms, NSA = 4, scan time: 5:19.

Ultrasonography

Ultrasonography was performed with a Philips CX50 at the start of the breeding period to confirm pregnancy. Once the females were confirmed pregnant, a minimum of biweekly ultrasounds were performed to determine gestational age and estimated parturition. Initial measurements consisted of anteroposterior and longitudinal measurements of the gestational sac. Once the fetus was more developed and the biparietal (BPD) measurements could be obtained then BPD measurements were utilized to track the growth and determine gestational age.

Serum antibody binding kinetics by surface plasmon resonance assay

Steady-state equilibrium binding of longitudinal polyclonal sera from every individual animal was monitored at 25°C using a ProteOn surface plasmon resonance (Bio Rad). The purified recombinant ZIKV proteins (ZIKV-E from Sino Biologicals and ZIKV-NS1 from Meridian Life Sciences) were coupled to a GLC sensor chip via amine coupling with either 100 or 500 resonance units (RU) in the test flow channels. The protein density on the chip was optimized such as to measure only monovalent interactions independent of the antibody isotype. Samples of 300 μl freshly prepared sera at 10-fold and 50- fold dilution in BSA-PBST buffer (PBS pH 7.4 buffer with Tween-20 and BSA) were injected at a flow rate of 50 μL/min (120 sec contact duration) for association, and disassociation was performed over a 600-second interval. Secondary anti-isotype antibodies were purified to remove cross-reactivity between isotypes by Brookwood Biomedical. Responses from the

protein surface were corrected for the response from a mock surface and for responses from a buffer-only injection. The maximum resonance units (Max RU) for each sample were calculated by multiplying the observed RU signal with the dilution factor to provide the data for an undiluted sample. Total antibody binding and antibody isotype analysis were calculated with BioRad ProteOn manager software (version 3.1.0). All SPR experiments were performed twice, and the researcher performing the assay was blinded to sample identity. In these optimized SPR conditions, the variation for each sample in duplicate SPR runs was <5%. The limit of detection was 20 RU.

Antigen-specific leukocyte stimulation

Peripheral blood mononuclear cells isolated from $E2_D$ at 23 dpi and from all infants −34 days prior to reinfections were plated in a 96 well plate at 250,000–350,000 cells per well. Cells were rested overnight prior to re-stimulation. Cells were stimulated in triplicate with 1ng/mL each of PepMix ZIKV (E) Ultra and PepMix ZIKV (NS1) Ultra (JPT Innovative Peptide Solutions, Acton, MA) or DMSO as a control for 2 hours prior to the addition of 10ug of Brefeldin A (Sigma Aldrich, St. Louis, MO) for an additional 4 hours. Cells were then transferred to FACS tubes for staining. Cells were stained first with LIVE/DEAD™ Fixable Blue Dead Cell Stain Kit (Invitrogen) for viability. Cells were then stained with the following fluorochrome conjugated antibodies: CD95 BUV737 (DX2), CD4 BV421 (L200), CD3 AF750 (SP34–2) (all from BD Biosciences, San Jose, CA) and CD8 BV605 (RPA-T8) from Biolegend (San Diego, CA). Cells were then fixed and permeabilized using the Cytofix/Cytoperm kit from BD Biosciences, followed staining with intracellular antibodies IFN-γ FITC (4S.B3) and TNF-α PE (MAb11) from BD Biosciences. Stained PBMCs were acquired on a BD FACSymphony (BD Biosciences, San Jose, CA) and analysis was completed using FlowJo software v10.5.3 (TreeStar, Ashland, OR).

ZIKV reporter virus particle neutralization and antibody dependent enhancement assay

Reporter virus particles (RVPs) incorporating the structural proteins of ZIKV (strain H/PF/2013) were produced by complementation of a sub-genomic GFP-expressing replicon derived from a lineage II strain of WNV as previously described(37). Briefly, HEK-293T cells were transfected with plasmids encoding the replicon and structural genes at a 1:3 ratio by mass using Lipofectamine 300 (Invitrogen), followed by incubation at 30°C. RVP-containing supernatant was harvested from cells at days 3–6 post-transfection, filtered through a 0.22 μm filter, and stored at −80°C. To determine virus titer, two-fold dilutions of RVPs were used to infect Raji cells that express the flavivirus attachment factor DC-SIGNR (Raji-DCSIGNR) in duplicate technical replicates at 37°C. GFP-positive infected cells were detected by flow cytometry 2 days later. In subsequent neutralization and antibody-dependent enhancement assays, RVPs were sufficiently diluted to within the linear range of the virus-infectivity dose-response curve to ensure antibody excess at informative points. For neutralization studies, ZIKV RVPs were mixed with serial dilutions of heat-inactivated macaque plasma for 1 h at 37°C, followed by infection of Raji-DCSIGNR cells in duplicate technical replicates. Infections were carried out at 37°C and GFP-positive infected cells quantified by flow cytometry 2 days later. Results were analyzed by non-linear regression analysis to estimate the dilution of plasma required to inhibit 50% of infection (EC50). For ADE studies, the assay was performed as described above except K562 cells that express

the Fc-γ receptor CD32A were used as the target cells for infection. Infectivity >3-fold over background was considered positive for ADE. For both neutralization and ADE, all samples were initially tested at a starting dilution of 1:60 (based on the final volume of cells, virus, and plasma per well), which was designated as the limit of detection. Negative values were reported as one half the limit of detection (1:30).

Statistical analysis

Significant differences in the data were determined by a two-tailed Student *t* test. A p-value <0.05 was deemed significant. Graphing and statistical analysis were performed using GraphPad Prism software.

Supplementary Material

Refer to Web version on PubMed Central for supplementary material.

Acknowledgements

We thank the Mouse Imaging Facility/NIH for help with MRI. We thank Sanhita Sinharary and William Schreiber-Stainthorp for help with obtaining the MR images. We also thank Jens Wrammert and Grace Mantus (Emory University) for their gracious assistance with the antibody-dependent enhancement assay, and Kelly Byrne for assistance with figures.

Funding:

This study was funded and supported by the Intramural Research Program of the National Institutes of Health, Clinical Center and National Institute of Allergy and Infectious Diseases. The antibody characterization was supported by U.S. Food and Drug Administration Medical Countermeasures Initiative funds provided to S.K. The funders had no role in the study design or data collection and analysis.

Data and Materials Availability:

All data associated with this study are in the main paper or supplementary materials.

References and Notes

1. Zika: the continuing threat. Bull World Health Organ 97, 6–7 (2019). [PubMed: 30618459]
2. Baud D, Gubler DJ, Schaub B, Lanteri MC, Musso D, An update on Zika virus infection. Lancet 390, 2099–2109 (2017). [PubMed: 28647173]
3. Grubaugh ND, Saraf S, Gangavarapu K, Watts A, Tan AL, Oidtman RJ, Ladner JT, Oliveira G, Matteson NL, Kraemer MUG, Vogels CBF, Hentoff A, Bhatia D, Stanek D, Scott B, Landis V, Stryker I, Cone MR, Kopp E. W. t., Cannons AC, Heberlein-Larson L, White S, Gillis LD, Ricciardi MJ, Kwal J, Lichtenberger PK, Magnani DM, Watkins DI, Palacios G, Hamer DH, N. GeoSentinel Surveillance, Gardner LM, Perkins TA, Baele G, Khan K, Morrison A, Isern S,Michael SF, Andersen KG, Travel Surveillance and Genomics Uncover a Hidden Zika Outbreak during the Waning Epidemic. Cell 178, 1057–1071 e1011 (2019). [PubMed: 31442400]
4. Rice ME, Galang RR, Roth NM, Ellington SR, Moore CA, Valencia-Prado M, Ellis EM, Tufa AJ, Taulung LA, Alfred JM, Perez-Padilla J, Delgado-Lopez CA, Zaki SR, Reagan-Steiner S, Bhatnagar J, Nahabedian JF 3rd, Reynolds MR, Yeargin-Allsopp M, Viens LJ, Olson SM, Jones AM, Baez-Santiago MA, Oppong-Twene P, VanMaldeghem K, Simon EL, Moore JT, Polen KD, Hillman B, Ropeti R, Nieves-Ferrer L, Marcano-Huertas M, Masao CA, Anzures EJ, Hansen RL Jr., Perez-Gonzalez SI, Espinet-Crespo CP, Luciano-Roman M, Shapiro-Mendoza CK, Gilboa SM, Honein MA, Vital Signs: Zika-Associated Birth Defects and Neurodevelopmental Abnormalities

Possibly Associated with Congenital Zika Virus Infection - U.S. Territories and Freely Associated States, 2018. MMWR Morb Mortal Wkly Rep 67, 858–867 (2018). [PubMed: 30091967]

5. Franca GV, Schuler-Faccini L, Oliveira WK, Henriques CM, Carmo EH, Pedi VD, Nunes ML, Castro MC, Serruya S, Silveira MF, Barros FC, Victora CG, Congenital Zika virus syndrome in Brazil: a case series of the first 1501 livebirths with complete investigation. Lancet 388, 891–897 (2016). [PubMed: 27372398]
6. Miranda-Filho Dde B, Martelli CM, Ximenes RA, Araujo TV, Rocha MA, Ramos RC, Dhalia R, Franca RF, Marques Junior ET, Rodrigues LC, Initial Description of the Presumed Congenital Zika Syndrome. Am J Public Health 106, 598–600 (2016). [PubMed: 26959258]
7. Pierson TC, Diamond MS, The emergence of Zika virus and its new clinical syndromes. Nature 560, 573–581 (2018). [PubMed: 30158602]
8. van der Linden V, Pessoa A, Dobyns W, Barkovich AJ, Junior HV, Filho EL, Ribeiro EM, Leal MC, Coimbra PP, Aragao MF, Vercosa I, Ventura C, Ramos RC, Cruz DD, Cordeiro MT, Mota VM, Dott M, Hillard C, Moore CA, Description of 13 Infants Born During October 2015-January 2016 With Congenital Zika Virus Infection Without Microcephaly at Birth - Brazil. MMWR Morb Mortal Wkly Rep 65, 1343–1348 (2016). [PubMed: 27906905]
9. Broussard CS, Shapiro-Mendoza CK, Peacock G, Rasmussen SA, Mai CT, Petersen EE, Galang RR, Newsome K, Reynolds MR, Gilboa SM, Boyle CA, Moore CA, Public Health Approach to Addressing the Needs of Children Affected by Congenital Zika Syndrome. Pediatrics 141, S146–S153 (2018). [PubMed: 29437047]
10. Chu V, Petersen LR, Moore CA, Meaney-Delman D, Nelson G, Christian Sonne D, Dodge NN, Glaser C, Rasmussen SA, Possible Congenital Zika Syndrome in Older Children Due to Earlier Circulation of Zika Virus. Am J Med Genet A 176, 1882–1889 (2018). [PubMed: 30070773]
11. Pessoa A, van der Linden V, Yeargin-Allsopp M, Carvalho M, Ribeiro EM, Van Naarden Braun K, Durkin MS, Pastula DM, Moore JT, Moore CA, Motor Abnormalities and Epilepsy in Infants and Children With Evidence of Congenital Zika Virus Infection. Pediatrics 141, S167–S179 (2018). [PubMed: 29437050]
12. Moura da Silva AA, Ganz JS, Sousa PD, Doriqui MJ, Ribeiro MR, Branco MD, Queiroz RC, Pacheco MJ, Vieira da Costa FR, Silva FS, Simoes VM, Pacheco MA, Lamy-Filho F, Lamy ZC, Soares de Britto EAMT, Early Growth and Neurologic Outcomes of Infants with Probable Congenital Zika Virus Syndrome. Emerg Infect Dis 22, 1953–1956 (2016). [PubMed: 27767931]
13. Satterfield-Nash A, Kotzky K, Allen J, Bertolli J, Moore CA, Pereira IO, Pessoa A, Melo F, Santelli A, Boyle CA, Peacock G, Health and Development at Age 19–24 Months of 19 Children Who Were Born with Microcephaly and Laboratory Evidence of Congenital Zika Virus Infection During the 2015 Zika Virus Outbreak - Brazil, 2017. MMWR Morb Mortal Wkly Rep 66, 1347–1351 (2017). [PubMed: 29240727]
14. Mohr EL, Modeling Zika Virus-Associated Birth Defects in Nonhuman Primates. J Pediatric Infect Dis Soc 7, S60–S66 (2018). [PubMed: 30590626]
15. Dudley DM, Aliota MT, Mohr EL, Newman CM, Golos TG, Friedrich TC, O'Connor DH, Using Macaques to Address Critical Questions in Zika Virus Research. Annu Rev Virol, (2019).
16. Simmons HA, Age-Associated Pathology in Rhesus Macaques (Macaca mulatta). Vet Pathol 53, 399–416 (2016). [PubMed: 26864889]
17. Colman RJ, Anderson RM, Johnson SC, Kastman EK, Kosmatka KJ, Beasley TM, Allison DB, Cruzen C, Simmons HA, Kemnitz JW, Weindruch R, Caloric restriction delays disease onset and mortality in rhesus monkeys. Science 325, 201–204 (2009). [PubMed: 19590001]
18. Osuna CE, Whitney JB, Nonhuman Primate Models of Zika Virus Infection, Immunity, and Therapeutic Development. J Infect Dis 216, S928–S934 (2017). [PubMed: 29267926]
19. Larocca RA, Abbink P, Peron JP, Zanotto PM, Iampietro MJ, Badamchi-Zadeh A, Boyd M, Ng'ang'a D, Kirilova M, Nityanandam R, Mercado NB, Li Z, Moseley ET, Bricault CA, Borducchi EN, Giglio PB, Jetton D, Neubauer G, Nkolola JP, Maxfield LF, De La Barrera RA, Jarman RG, Eckels KH, Michael NL, Thomas SJ, Barouch DH, Vaccine protection against Zika virus from Brazil. Nature 536, 474–478 (2016). [PubMed: 27355570]
20. Abbink P, Larocca RA, De La Barrera RA, Bricault CA, Moseley ET, Boyd M, Kirilova M, Li Z, Ng'ang'a D, Nanayakkara O, Nityanandam R, Mercado NB, Borducchi EN, Agarwal A, Brinkman

AL, Cabral C, Chandrashekar A, Giglio PB, Jetton D, Jimenez J, Lee BC, Mojta S, Molloy K, Shetty M, Neubauer GH, Stephenson KE, Peron JP, Zanotto PM, Misamore J, Finneyfrock B, Lewis MG, Alter G, Modjarrad K, Jarman RG, Eckels KH, Michael NL, Thomas SJ, Barouch DH, Protective efficacy of multiple vaccine platforms against Zika virus challenge in rhesus monkeys. Science 353, 1129–1132 (2016). [PubMed: 27492477]

21. Magnani DM, Rogers TF, Beutler N, Ricciardi MJ, Bailey VK, Gonzalez-Nieto L, Briney B, Sok D, Le K, Strubel A, Gutman MJ, Pedreno-Lopez N, Grubaugh ND, Silveira CGT, Maxwell HS, Domingues A, Martins MA, Lee DE, Okwuazi EE, Jean S, Strobert EA, Chahroudi A, Silvestri G, Vanderford TH, Kallas EG, Desrosiers RC, Bonaldo MC, Whitehead SS, Burton DR, Watkins DI, Neutralizing human monoclonal antibodies prevent Zika virus infection in macaques. Sci Transl Med 9, (2017).
22. Van Rompay KKA, Keesler RI, Ardeshir A, Watanabe J, Usachenko J, Singapuri A, Cruzen C, Bliss-Moreau E, Murphy AM, Yee JL, Webster H, Dennis M, Singh T, Heimsath H, Lemos D, Stuart J, Morabito KM, Foreman BM, Burgomaster KE, Noe AT, Dowd KA, Ball E, Woolard K, Presicce P, Kallapur SG, Permar SR, Foulds KE, Coffey LL, Pierson TC, Graham BS, DNA vaccination before conception protects Zika virus-exposed pregnant macaques against prolonged viremia and improves fetal outcomes. Sci Transl Med 11, (2019).
23. Magnani DM, Rogers TF, Maness NJ, Grubaugh ND, Beutler N, Bailey VK, Gonzalez-Nieto L, Gutman MJ, Pedreno-Lopez N, Kwal JM, Ricciardi MJ, Myers TA, Julander JG, Bohm RP, Gilbert MH, Schiro F, Aye PP, Blair RV, Martins MA, Falkenstein KP, Kaur A, Curry CL, Kallas EG, Desrosiers RC, Goldschmidt-Clermont PJ, Whitehead SS, Andersen KG, Bonaldo MC, Lackner AA, Panganiban AT, Burton DR, Watkins DI, Fetal demise and failed antibody therapy during Zika virus infection of pregnant macaques. Nat Commun 9, 1624 (2018). [PubMed: 29691387]
24. Mold JE, Michaelsson J, Burt TD, Muench MO, Beckerman KP, Busch MP, Lee TH, Nixon DF, McCune JM, Maternal alloantigens promote the development of tolerogenic fetal regulatory T cells in utero. Science 322, 1562–1565 (2008). [PubMed: 19056990]
25. Odorizzi PM, Jagannathan P, McIntyre TI, Budker R, Prahl M, Auma A, Burt TD, Nankya F, Nalubega M, Sikyomu E, Musinguzi K, Naluwu K, Kakuru A, Dorsey G, Kamya MR, Feeney ME, In utero priming of highly functional effector T cell responses to human malaria. Sci Transl Med 10, (2018).
26. Simon AK, Hollander GA, McMichael A, Evolution of the immune system in humans from infancy to old age. Proc Biol Sci 282, 20143085 (2015). [PubMed: 26702035]
27. Zhang X, Mozeleski B, Lemoine S, Deriaud E, Lim A, Zhivaki D, Azria E, Le Ray C, Roguet G, Launay O, Vanet A, Leclerc C, Lo-Man R, CD4 T cells with effector memory phenotype and function develop in the sterile environment of the fetus. Sci Transl Med 6, 238ra272 (2014).
28. Zhivaki D, Lo-Man R, In utero development of memory T cells. Semin Immunopathol 39, 585–592 (2017). [PubMed: 28900758]
29. Wilcox CR, Jones CE, Beyond Passive Immunity: Is There Priming of the Fetal Immune System Following Vaccination in Pregnancy and What Are the Potential Clinical Implications? Front Immunol 9, 1548 (2018). [PubMed: 30061881]
30. Shapiro-Mendoza CK, Rice ME, Galang RR, Fulton AC, VanMaldeghem K, Prado MV, Ellis E, Anesi MS, Simeone RM, Petersen EE, Ellington SR, Jones AM, Williams T, Reagan-Steiner S, Perez-Padilla J, Deseda CC, Beron A, Tufa AJ, Rosinger A, Roth NM, Green C, Martin S, Lopez CD, deWilde L, Goodwin M, Pagano HP, Mai CT, Gould C, Zaki S, Ferrer LN, Davis MS, Lathrop E, Polen K, Cragan JD, Reynolds M, Newsome KB, Huertas MM, Bhatangar J, Quinones AM, Nahabedian JF, Adams L, Sharp TM, Hancock WT, Rasmussen SA, Moore CA, Jamieson DJ, Munoz-Jordan JL, Garstang H, Kambui A, Masao C, Honein MA, Meaney-Delman D, Zika P, G. Infant Registries Working, Pregnancy Outcomes After Maternal Zika Virus Infection During Pregnancy - U.S. Territories, January 1, 2016-April 25, 2017. MMWR Morb Mortal Wkly Rep 66, 615–621 (2017). [PubMed: 28617773]
31. Kleber de Oliveira W, Cortez-Escalante J, De Oliveira WT, do Carmo GM, Henriques CM, Coelho GE, Araujo de Franca GV, Increase in Reported Prevalence of Microcephaly in Infants Born to Women Living in Areas with Confirmed Zika Virus Transmission During the First Trimester of Pregnancy - Brazil, 2015. MMWR Morb Mortal Wkly Rep 65, 242–247 (2016). [PubMed: 26963593]

32. Krow-Lucal ER, de Andrade MR, Cananea JNA, Moore CA, Leite PL, Biggerstaff BJ, Cabral CM, Itoh M, Percio J, Wada MY, Powers AM, Barbosa A, Abath RB, Staples JE, Coelho GE, G. Paraiba Microcephaly Work, Association and birth prevalence of microcephaly attributable to Zika virus infection among infants in Paraiba, Brazil, in 2015–16: a case-control study. Lancet Child Adolesc Health 2, 205–213 (2018). [PubMed: 30169255]
33. Tarantal AF, Laboratory Primate. (Elsevier Academic Press, Amsterdam, 2005).
34. Schneider ML, Suomi SJ, Neurobehavioral assessment in rhesus monkey neonates (Macaca mulatta): developmental changes, behavioral stability, and early experience. Infant Behavior and Development 15, 155–177 (1992).
35. Nguyen SM, Antony KM, Dudley DM, Kohn S, Simmons HA, Wolfe B, Salamat MS, Teixeira LBC, Wiepz GJ, Thoong TH, Aliota MT, Weiler AM, Barry GL, Weisgrau KL, Vosler LJ, Mohns MS, Breitbach ME, Stewart LM, Rasheed MN, Newman CM, Graham ME, Wieben OE, Turski PA, Johnson KM, Post J, Hayes JM, Schultz-Darken N, Schotzko ML, Eudailey JA, Permar SR, Rakasz EG, Mohr EL, Capuano S 3rd, Tarantal AF, Osorio JE, O'Connor SL, Friedrich TC, O'Connor DH, Golos TG, Highly efficient maternal-fetal Zika virus transmission in pregnant rhesus macaques. PLoS Pathog 13, e1006378 (2017). [PubMed: 28542585]
36. Carroll SL, Worley SH, in Reference Module in Neuroscience and Biobehavioral Psychology. (Medical University of South Carolina, Charleston, SC, USA, 2017).
37. Dowd KA, DeMaso CR, Pelc RS, Speer SD, Smith ARY, Goo L, Platt DJ, Mascola JR, Graham BS, Mulligan MJ, Diamond MS, Ledgerwood JE, Pierson TC, Broadly Neutralizing Activity of Zika Virus-Immune Sera Identifies a Single Viral Serotype. Cell Rep 16, 1485–1491 (2016). [PubMed: 27481466]
38. Dowd KA, Ko SY, Morabito KM, Yang ES, Pelc RS, DeMaso CR, Castilho LR, Abbink P, Boyd M, Nityanandam R, Gordon DN, Gallagher JR, Chen X, Todd JP, Tsybovsky Y, Harris A, Huang YS, Higgs S, Vanlandingham DL, Andersen H, Lewis MG, De La Barrera R, Eckels KH, Jarman RG, Nason MC, Barouch DH, Roederer M, Kong WP, Mascola JR, Pierson TC, Graham BS, Rapid development of a DNA vaccine for Zika virus. Science 354, 237–240 (2016). [PubMed: 27708058]
39. DeSesso JM, Williams AL, Ahuja A, Bowman CJ, Hurtt ME, The placenta, transfer of immunoglobulins, and safety assessment of biopharmaceuticals in pregnancy. Crit Rev Toxicol 42, 185–210 (2012). [PubMed: 22348352]
40. Shen C, Xu H, Liu D, Veazey RS, Wang X, Development of serum antibodies during early infancy in rhesus macaques: implications for humoral immune responses to vaccination at birth. Vaccine 32, 5337–5342 (2014). [PubMed: 25092633]
41. Hurley WL, Theil PK, Perspectives on immunoglobulins in colostrum and milk. Nutrients 3, 442–474 (2011). [PubMed: 22254105]
42. Leong KW, Ding JL, The unexplored roles of human serum IgA. DNA Cell Biol 33, 823–829 (2014). [PubMed: 25188736]
43. Zhao LZ, Hong WX, Wang J, Yu L, Hu FY, Qiu S, Yin CB, Tang XP, Zhang LQ, Jin X, Zhang FC, Kinetics of antigen-specific IgM/IgG/IgA antibody responses during Zika virus natural infection in two patients. J Med Virol 91, 872–876 (2019). [PubMed: 30485459]
44. Warnecke JM, Lattwein E, Saschenbrecker S, Stocker W, Schlumberger W, Steinhagen K, Added value of IgA antibodies against Zika virus non-structural protein 1 in the diagnosis of acute Zika virus infections. J Virol Methods 267, 8–15 (2019). [PubMed: 30779938]
45. Maness NJ, Schouest B, Singapuri A, Dennis M, Gilbert MH, Bohm RP, Schiro F, Aye PP, Baker K, Van Rompay KKA, Lackner AA, Bonaldo MC, Blair RV, Permar SR, Coffey LL, Panganiban AT, Magnani D, Postnatal Zika virus infection of nonhuman primate infants born to mothers infected with homologous Brazilian Zika virus. Sci Rep 9, 12802 (2019). [PubMed: 31488856]
46. Mavigner M, Raper J, Kovacs-Balint Z, Gumber S, O'Neal JT, Bhaumik SK, Zhang X, Habib J, Mattingly C, McDonald CE, Avanzato V, Burke MW, Magnani DM, Bailey VK, Watkins DI, Vanderford TH, Fair D, Earl E, Feczko E, Styner M, Jean SM, Cohen JK, Silvestri G, Johnson RP, O'Connor DH, Wrammert J, Suthar MS, Sanchez MM, Alvarado MC, Chahroudi A, Postnatal Zika virus infection is associated with persistent abnormalities in brain structure, function, and behavior in infant macaques. Sci Transl Med 10, (2018).

47. Aliota MT, Dudley DM, Newman CM, Mohr EL, Gellerup DD, Breitbach ME, Buechler CR, Rasheed MN, Mohns MS, Weiler AM, Barry GL, Weisgrau KL, Eudailey JA, Rakasz EG, Vosler LJ, Post J, Capuano S 3rd, Golos TG, Permar SR, Osorio JE, Friedrich TC, O'Connor SL, O'Connor DH, Heterologous Protection against Asian Zika Virus Challenge in Rhesus Macaques. PLoS Negl Trop Dis 10, e0005168 (2016). [PubMed: 27911897]

48. Dudley DM, Aliota MT, Mohr EL, Weiler AM, Lehrer-Brey G, Weisgrau KL, Mohns MS, Breitbach ME, Rasheed MN, Newman CM, Gellerup DD, Moncla LH, Post J, Schultz-Darken N, Schotzko ML, Hayes JM, Eudailey JA, Moody MA, Permar SR, O'Connor SL, Rakasz EG, Simmons HA, Capuano S, Golos TG, Osorio JE, Friedrich TC, O'Connor DH, A rhesus macaque model of Asian-lineage Zika virus infection. Nat Commun 7, 12204 (2016). [PubMed: 27352279]

49. Yanai T, Masegi T, Ueda K, Manabe J, Teranishi M, Takaoka M, Matsunuma N, Fukuda K, Goto N, Fujiwara K, Vascular mineralization in the monkey brain. Vet Pathol 31, 546–552 (1994). [PubMed: 7801432]

50. Winkler CW, Woods TA, Rosenke R, Scott DP, Best SM, Peterson KE, Sexual and Vertical Transmission of Zika Virus in anti-interferon receptor-treated Rag1-deficient mice. Sci Rep 7, 7176 (2017). [PubMed: 28775298]

51. Winkler CW, Race B, Phillips K, Peterson KE, Capillaries in the olfactory bulb but not the cortex are highly susceptible to virus-induced vascular leak and promote viral neuroinvasion. Acta Neuropathol 130, 233–245 (2015). [PubMed: 25956408]

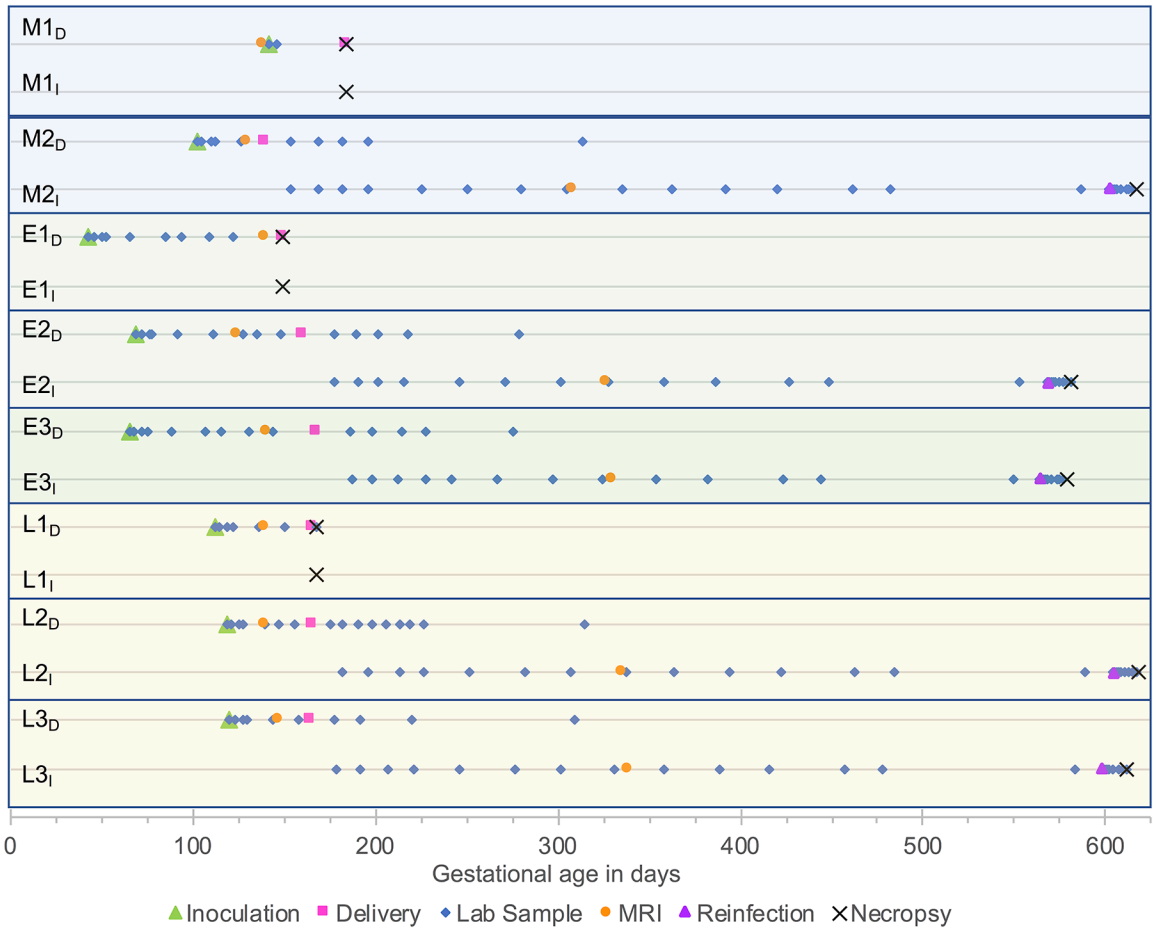

Figure 1. Study timeline.

Shown is the study timeline for ZIKV infection of rhesus macaque dams, delivery of offspring, blood and cerebrospinal fluid sampling, MRI, reinfection of offspring with ZIKV at 13–15 months of age, and necropsy. M, mock-infected; E, early gestational infection; L, late gestational infection; D, dam; I, infant offspring. The first dam and infant pair from each cohort were euthanized at the time of delivery and their tissues were analyzed. The remainder of the infants were observed for the entirety of the study.

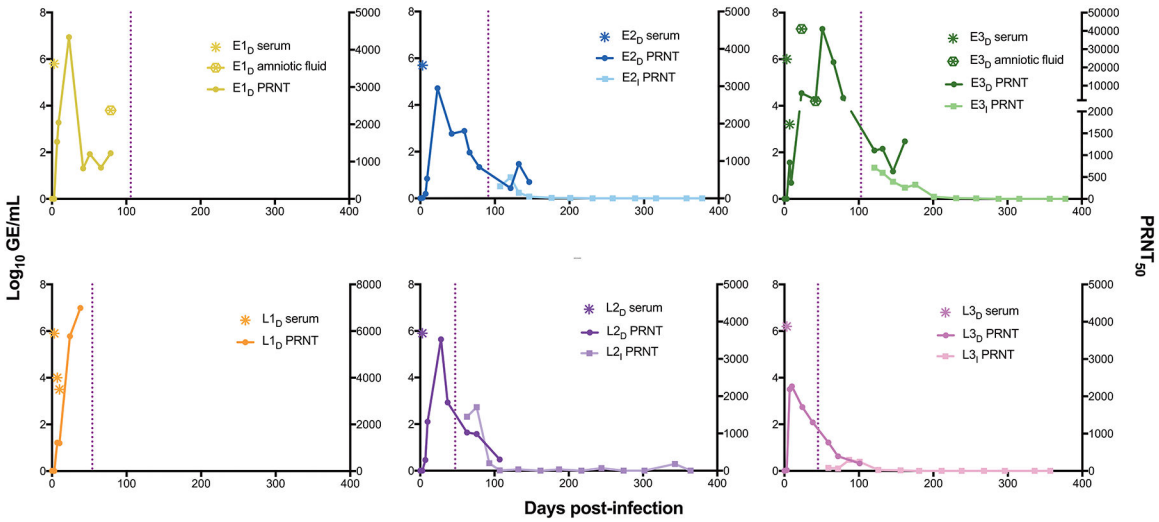

Figure 2. ZIKV in fluid samples from ZIKV-infected dams and their infants.

Serum and amniotic fluid samples were obtained prenatally and postnatally at different time points after infection of macaque dams with ZIKV. Samples were assayed for ZIKV RNA (Log_{10} GE/ml) by qPCR; negative ZIKV RNA readings are not shown. Total ZIKV-specific neutralizing antibodies in serum are represented by the dilution that achieved a 50% reduction in viral plaques ($PRNT_{50}$ test). All $PRNT_{50}$ positive and negative readings are shown. The vertical dotted line indicates time of birth for offspring. All ZIKV-infected dam-infant pairs are shown. All ZIKV RNA and $PRNT_{50}$ measurements from the mock-infected dam-infant pairs were below the limit of detection.

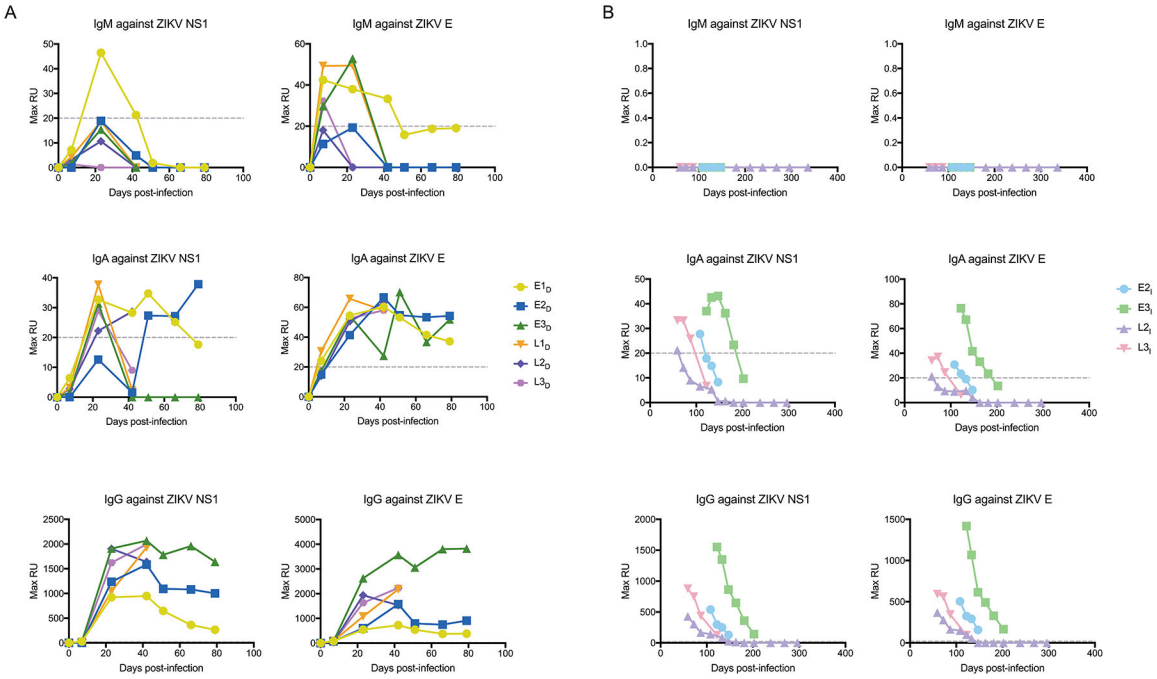

Figure 3. Antibody isotype kinetics in blood samples from macaque dams and infant offspring.

Shown are the kinetics of IgM, IgA, and IgG antibodies against ZIKV envelope (E) protein and NS1 protein in blood samples from ZIKV-infected dams **(A)** and their infant offspring **(B).** Antibody binding to ZIKV protein-coated sensors was detected by surface plasmon resonance and is expressed as maximum relative units (Max RU). Max RU was calculated by multiplying the observed RU signal by dilution factors. The dashed line indicates the lower limit of detection for the assay. E, early gestational infection; L, late gestational infection; D, dam; I, infant offspring.

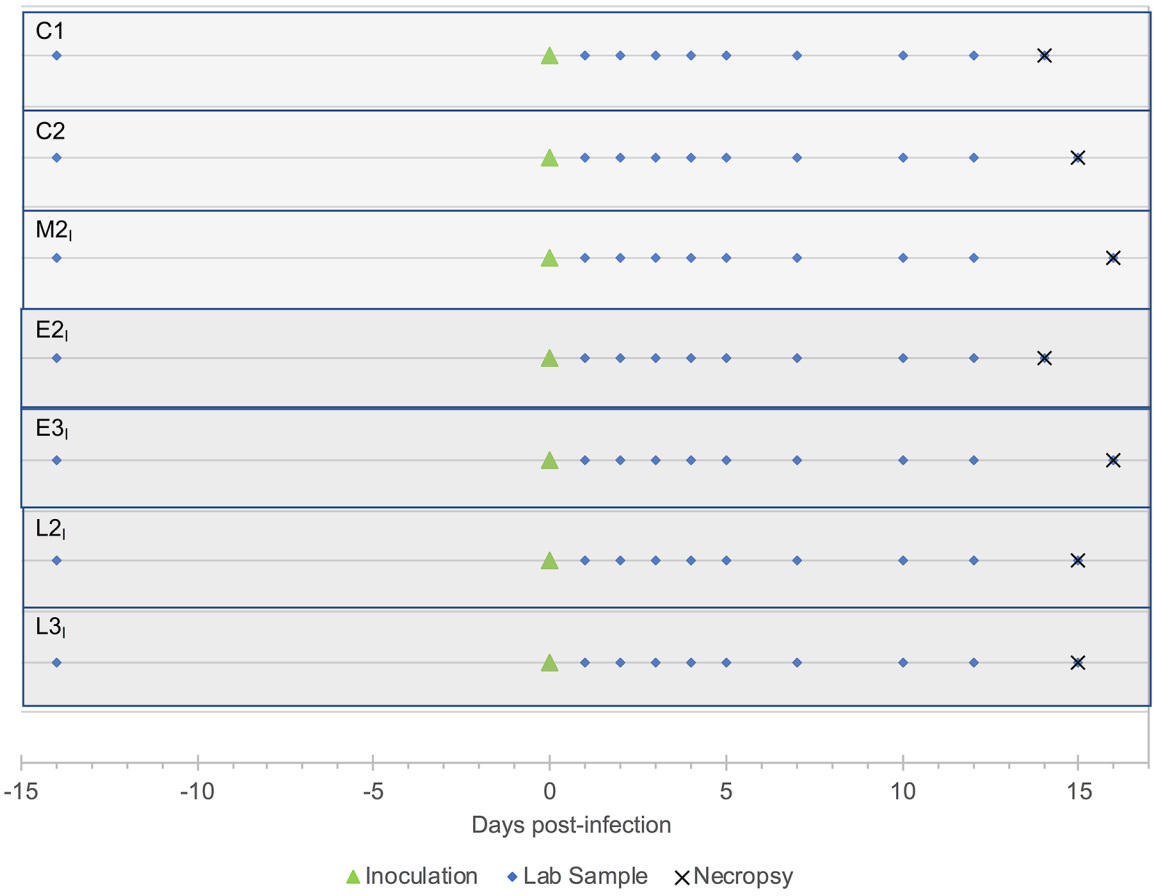

Figure 4. Timeline for the ZIKV reinfection study.

Two cohorts of animals were used in this study: the first comprised offspring born to dams that were not infected with ZIKV during pregnancy (15-month-old $M2_I$ and two additional two-year-old animals, C1 and C2), and the second cohort comprised the four 13–15-month-old offspring ($E2_I$, $E3_I$, $L2_I$, $L3_I$) born to dams that were infected with ZIKV while pregnant. All seven macaques were inoculated with the same strain and dose of ZIKV used for the primary infection (green triangle). Blood samples were taken at 1, 2, 3, 4, 5, 7, 10 and 12 days after inoculation (blue triangles). Cerebrospinal fluid was collected on days −14 (2 weeks before reinfection), 3 and 7 days after reinfection and at necropsy (blue triangles). Necropsies were performed 14–16 days after ZIKV reinfection. M, a macaque infant born to a dam mock-infected while pregnant; E, macaque infants born to dams infected with ZIKV during early gestation; L, macaque infants born to dams infected with ZIKV during late gestation; I, infant offspring.

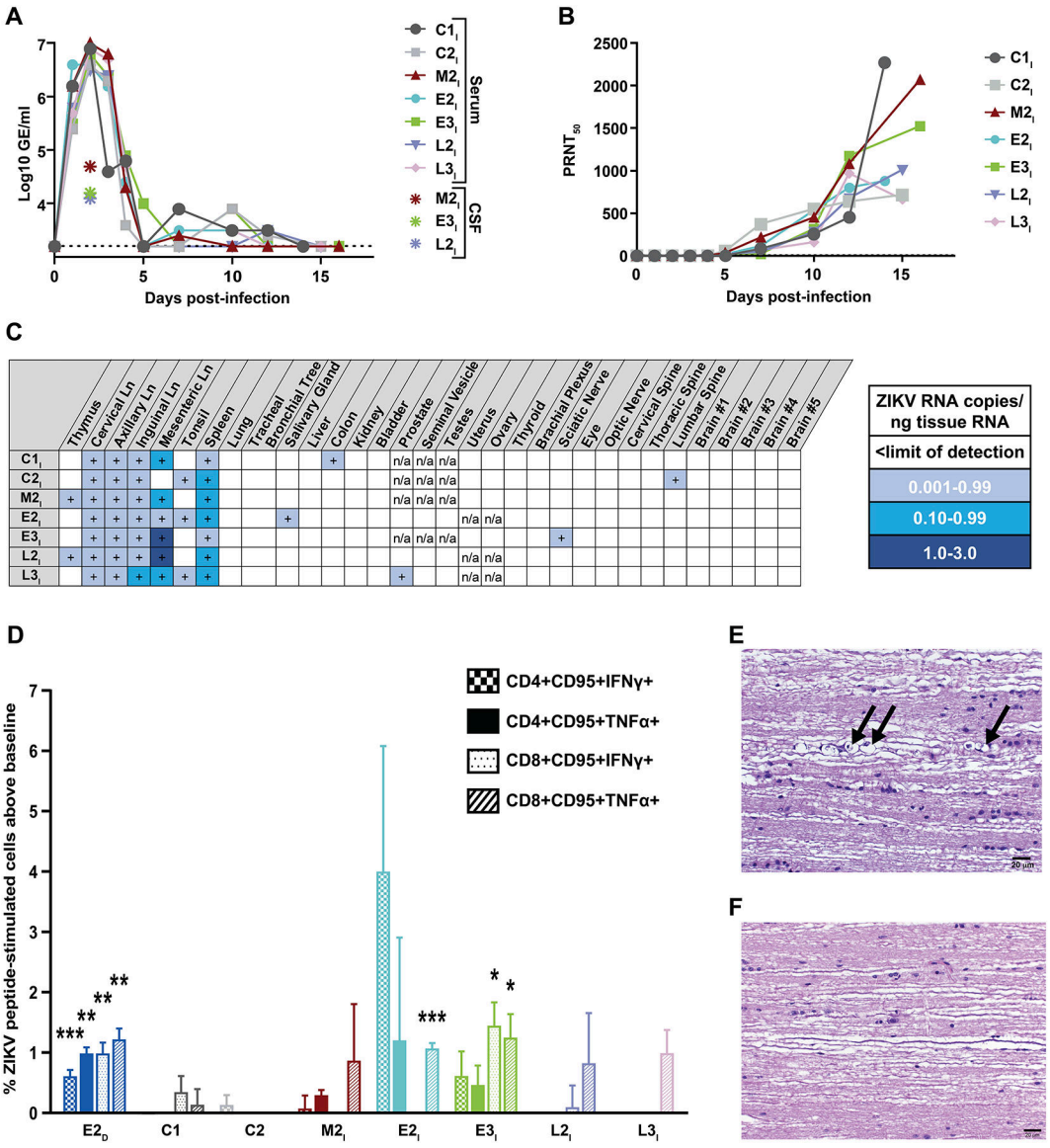

Figure 5. Anti-viral immune responses after ZIKV reinfection of macaque offspring.

(**A**) ZIKV RNA (Log_{10} GE/ml) was quantified by qPCR in serum and cerebrospinal fluid (CSF) of $M2_I$, C1 and C2 macaques (cohort 1, no prior ZIKV exposure), and $E2_I$, $E3_I$, $L2_I$, $L3_I$ (cohort 2, 13–15-month-old offspring born to dams infected with ZIKV while pregnant). Results for all serum samples are shown. Only positive CSF measurements are indicated. The dotted line marks the limit of detection of the assay. (**B**) Shown are the amounts of total ZIKV-specific neutralizing antibodies in blood samples from the seven macaques represented by the dilution that achieved a 50% reduction in viral plaques ($PRNT_{50}$ test). All $PRNT_{50}$ data are shown. (**C**) Quantification by droplet digital PCR of ZIKV RNA in lymphoid, pulmonary, digestive, genitourinary and nervous system tissues from the two cohorts is presented. (**D**) Shown are ZIKV-specific T cell memory responses in blood samples from the seven macaques as well as a single dam infected during early pregnancy ($E2_D$) measured by flow cytometry. Infant samples ($E2_I$, $E3_I$, $L2_I$, $L3_I$) were collected 30

days before the reinfection study; the dam sample was collected 23 days after inoculation with ZIKV during pregnancy. Data are presented as the percentage of cytokine-positive T cells after stimulation of PBMCs with ZIKV envelope and NS1 peptides (with subtraction of baseline, which is the percentage of the same cells producing cytokines without stimulation). Statistically significant differences between the peptide stimulated (N=3 technical replicates for each cell/cytokine combination) and unstimulated groups (N=3 technical replicates) were determined by Student's *t* test (*p<0.05, **p<0.01, ***p<0.001). Data shown are mean +/− SEM. (E) Shown is a representative thoracic spinal cord section from infant $E3_I$ stained with hematoxylin and eosin showing mineralized lesions after ZIKV reinfection. Wallerian degeneration associated with digestion chambers in the cytoplasm of Schwann cells is indicated by black arrows. (F) Shown is a representative normal thoracic spinal cord section from infant $M2_I$ stained with hematoxylin and eosin. Scale bar is 20 μm.